Proc. Natl. Sci. Counc. ROC(A)
Vol. 21, No. 2, 1997. pp. 113-125

Mechanical Characteristics of Flat Shaped Hydraulic Fill Sand

CHIEN-CHUNG LI AND CHING-JIANG JENG†

Department of Civil Engineering
National Central University
Chung Li, Taiwan, R.O.C.

(Received June 26, 1995; Accepted December 20, 1996)

ABSTRACT

Many large scale offshore reclamation projects are now in the planning stage in Taiwan. Most of these projects will involve the use of hydraulic fill techniques. The need for research related to land reclamation technology has become more obvious in Taiwan, especially for reclamation engineering near the seashore using dredging and hydraulic fill techniques.

In this research, a sand-water mixture transportation device has been developed to prepare testing samples. The behavior of the deposition process is evaluated in detail, and a steady state line series and the correlation between the state parameter and mechanical properties of hydraulic fill sand are investigated. It is observed that the salinity of the pore fluid has no effect on the steady state line. In triaxial and axial compressive shearing tests, the steady state line obtained from wet tamping specimens showed lower strength than did that of specimens created by hydraulic transportation. The axial extension test had lower strength than did the axial compression test. This difference was due to the influence of fabric orientation with respect to principal stress direction. The correlation curves between engineering properties and state parameters obtained from different sands under different states appear to exhibit a similar trend.

Key Words: hydraulic fill, flat shaped sand, mechanical properties, fabric, land reclamation, offshore engineering, state parameter

I. Introduction

There are many offshore land reclamation projects in the planning stage along the west coast of Taiwan, as shown in Fig. 1. Most of these projects will involve the use of hydraulic fill techniques. The need for research related to land reclamation technology has become more obvious, especially so for reclamation engineering near the seashore using dredging and hydraulic fill techniques.

Because of differences in the duration of the formation and deposition processes, hydraulic fill sand and naturally deposited soil are dissimilar in terms of engineering properties and mechanical behavior. Generally, hydraulic fill sand is loose especially for that under water. It is difficult to obtain reliable undisturbed samples for such sand. An indirect method, which correlates the results of laboratory simulation with the results of field tests, is commonly used (Been *et al.*, 1987) to determine the engineering properties of hydraulic fill sand. Relative density (D_r) has been widely used to describe the condition of in situ sandy soil. However, Li *et al.* (1991) and Been *et al.* (1987) have found that D_r only reflects the void ratio and has no obvious correlation with the stress state and volume change tendency, which are very much related to the strength and deformation characteristics for a granular soil. Been and Jefferies (1985) introduced the "State Parameter" to replace D_r in their study conducted for a reclamation project in the Canadian Beaufort Sea. The "State Parameter" is an index which combines D_r and the stress state into one parameter; thus, it can better describe the volume change tendency and the engineering characteristics for sandy soil.

Before applying the state parameter concept in practice, steady state lines, which are the basis of state parameters, should be established. Several factors influencing steady state lines have been discussed by Been *et al.* (1991) and Vaid *et al.* (1990). However, there are still some uncertainties and conflicting results

†All correspondence should be addressed to C.J. Jeng at Chung-Chi Technical Consultant Co., LTD 12F-1, No. 431, Kuang-Fu South Road, Taipei 106, Taiwan, R.O.C.

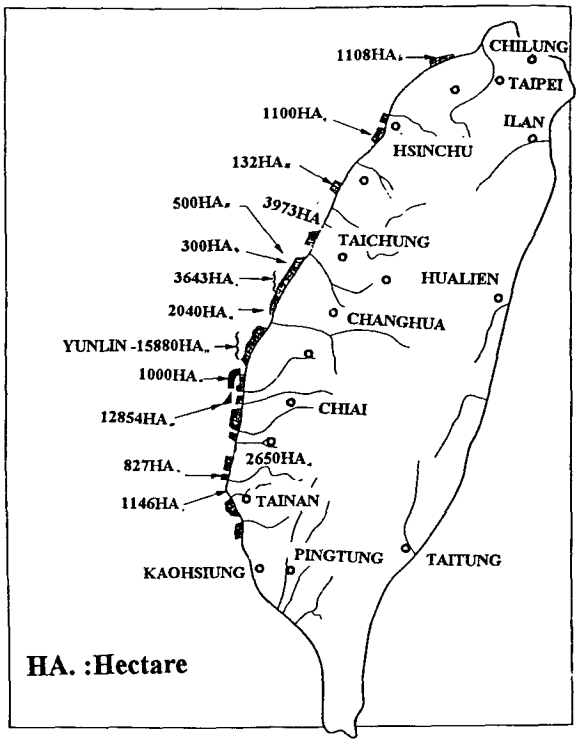

Fig. 1. Location of planned reclamation projects in the west coast of Taiwan.

between these two researches. For instance, Vaid *et al.* (1990) found that the stress path influences the steady state line; on the contrary, Been *et al.* (1991) deemed that the stress path has no effect on the steady state line. In addition, all the sands used by Been *et al.* had spherical particles, so it is necessary to verify whether the experiences obtained from spherical sand can be applied to flat sand. Moreover, the soil fabric formed by hydraulic fill may be quite different from the fabric of specimens used in the aforementioned studies. The aim of this research was to establish complete steady state lines of flat shaped hydraulic fill sand. Factors that are likely to influence steady state lines, such as the fines content, stress path, the method of specimen preparation, drainage conditions and pore fluids, are discussed in detail. Finally, image analysis of the soil fabric is conducted to verify the phenomenon observed in mechanical test results.

II. Materials and Testing Methods

1. Soil Properties

The sand used in this research was obtained from two sources; one the hydraulic-fill from Mai-liao, and the other was from the offshore seabed near Yunlin, where the sand is planned to be used as borrow material in the future. The physical properties of these two

Table 1. Physical Properties of Testing Soils

Testing Soils	Mailiao Sand	Yunlin Sand			
Fines Content	0%	0%	10%	20%	30%
Gs[a]	2.72	2.68	2.68	2.68	2.66
Cu[b]	1.92	1.6	2.4	3.0	4.7
$\gamma^{c}_{dmax(g/cm^3)}$	1.652	1.615	1.660	1.706	1.749
$\gamma^{d}_{dmin(g/cm^3)}$	1.247	1.212	1.211	1.191	1.175
D^{e}_{50}(mm)	0.190	0.151	0.143	0.133	0.122
USCS Classification	SP	SP	SP-SM	SM	SM

[a] specific gravity of soil particles.
[b] uniformity coefficient.
[c] maximum dry density.
[d] minimum dry density.
[e] particle diameter 50% finer than (median particle size).

Fig. 2. Particle shape of testing sand (No. 100-200 Sieve).

sands are summarized in Table 1. Particles of the testing soils were mostly flat with subrounded to subangular shapes, as shown in Fig. 2.

2. Specimen Preparation

In this study, a sand-water mixture transporting device was used to simulate the process of reclamation, which has been stated by Verhoeven *et al.* (1988) and includes loosening, mixing, transporting and settling. Sand is transported by hydraulic force, which induces circulation from the mixing tank to the settling column; at the same time, the particles which do not settle flow back to the mixing tank and are transported again. This procedure is repeated until adequate samples are obtained. At the bottom of the settling column, a split sampler was installed to form the testing specimen.

The simulation minimized possible disturbance

during sampling and withdrawing to maintain the original stacking fabric at completion of sand specimen formation. All of the stacking processes and variations of the slurry concentration during transportation were monitored, and the final distributions of the void ratio and particle gradation of the sample were also evaluated.

After the testing device was set up, water was circulated from the mixing tank to the settling column, and then the testing sand was poured into the mixing tank. The concentration of slurry in the mixing tank decreased gradually because the sand particles in the slurry deposited at the bottom of the column. The concentration ratio was defined as the ratio of the weight concentration of the sand at any time to the original concentration in the mixing tank. The difference in the concentration ratio between the slurry in the mixing tank and the slurry in the overflow pipe line is illustrated on Fig. 3, which shows that, after about ten minutes, the slope of curve became slower, and most of the sand particle had been transported to the settling column. The correlation equation showing the linear result after the first ten minutes with a correlation coefficient equals 0.991. From observation of the settling record, the testing specimen reached the anticipated height within ten minutes. The time span of the linear segment on the curve is dependent on the total amount of sand used in the test.

The maximum fines content of the samples was limited during preparation using sand-water mixture transportation. Thus, another group of samples was prepared by wet tamping with higher fines content to study the effects of fine particles.

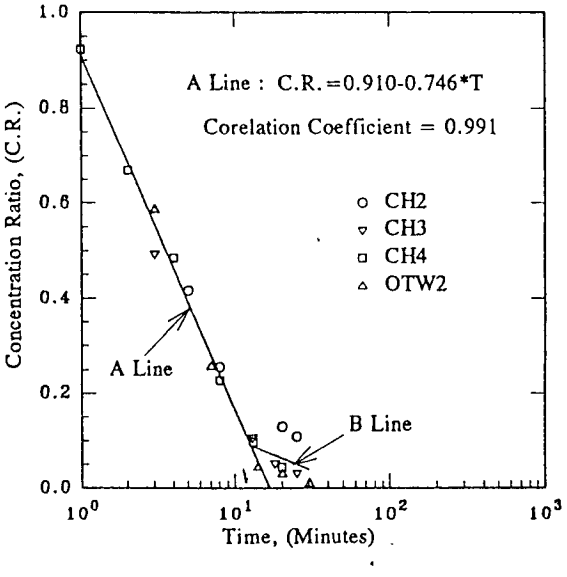

Fig. 3. Difference of concentration ratio between mixing tank and overflow lines.

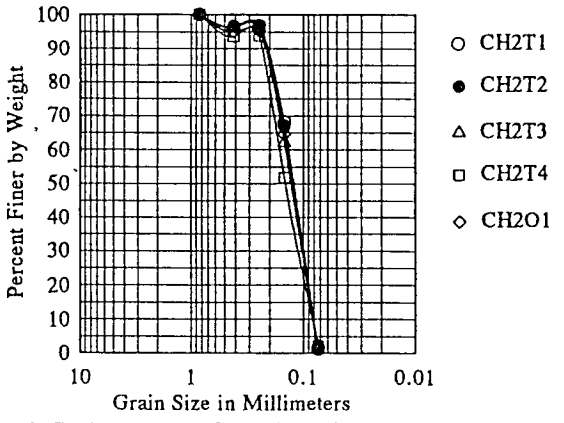

Fig. 4. Gradation curves for each specimen segment prepared using the hydraulic transportation method (Yunlin sand).

3. Physical Properties of the Samples

To study the particle distribution and density variation along with the depth of the sample as a result of hydraulic sand transportation, frozen specimens were cut into slices. The density and particle distribution of each slice were then determined separately. Figure 4 shows the results of the gradation curves of each slice for one set of Yunlin sand samples. The curves marked with CH2T1 to CH2T4 represent the gradation of the sample slice from top to bottom along the depth of the sample, and the segments were approximately equal in length. The curve marked CH2O1 represents the original condition of the testing sand. As indicated in the figures, the particle distribution curves of the slices are almost the same. In general, the sand grain size distribution was uniform, and no obvious particle segregation was found. The variation

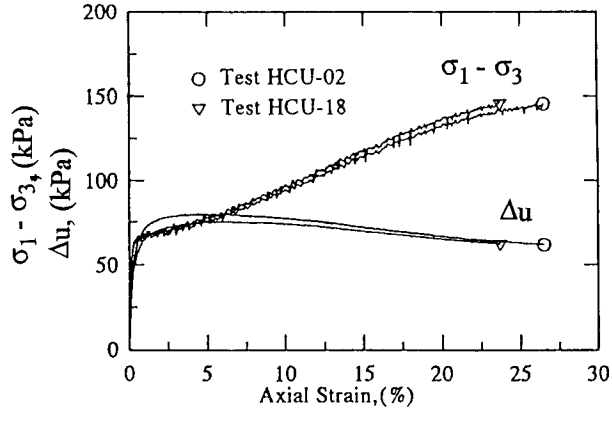

Fig. 5. Repeatability of specimens prepared using the hydraulic transportation method.

of density and relative density was less than 1% to 5%, respectively, among the segments. The value of relative density was obtained based on the maximum and minimum density of each segment. The range of the relative density value was from 14% to 60%, which is within the normal range of 10% to 70% for typical cases in the field (Sladen and Wemitt, 1989). In order to check the repeatability of the tests, two sets of samples prepared under the same conditions were used to compare their stress-strain curves and their generation of excess pore water pressure. As shown in Fig. 5, the void ratio of the specimen after consolidation was 0.955 and 0.946 (D_r=39.0% and 41.2%), respectively, for the same confining pressure of 98 kPa. It can be observed that the results for these two samples are similar. Based on these results, it can be concluded that samples prepared using the hydraulic transportation device in this research satisfied the requirements of uniformity and repeatability.

4. Drained and Undrained Triaxial Test Results

For a typical contractive soil, the results of the undrained triaxial test are shown in Fig. 6. Referring to Fig. 6(a), after the stress-strain curve passed peak point A, the deviator stress decreased continuously down to a residual deviator stress, which is marked as point B in the figure. The tendency of contraction in volume under shearing generated a positive excess pore water pressure, which is shown in Fig. 6(b). When the shear strain increased, excess pore water pressure

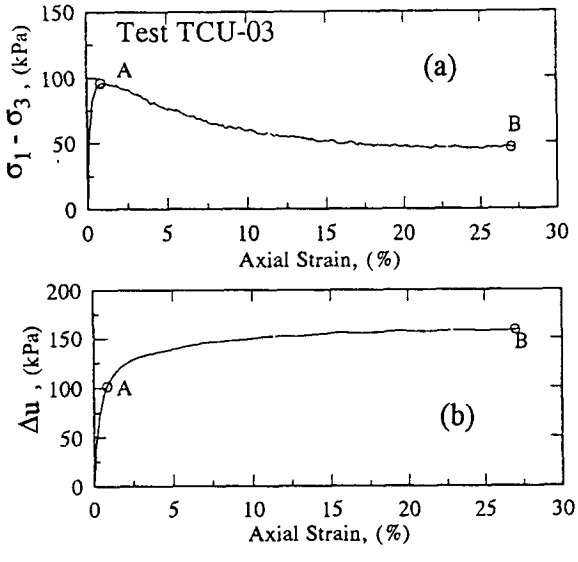

Fig. 6. Undrained triaxial test with contractive response (D_r=37.0%, σ'_c=196 kPa, ψ=0.112).

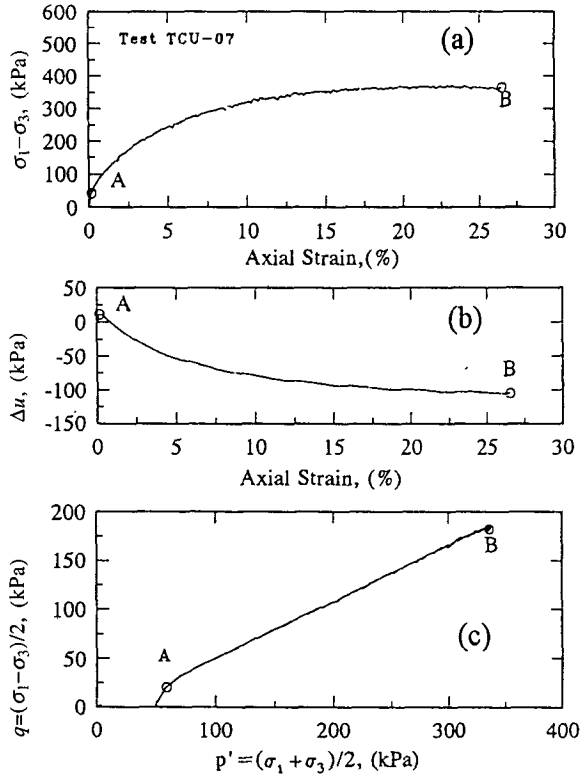

Fig. 7. Undrained triaxial test with dilative response (D_r=64.7%, σ'_c=49 kPa, ψ=−0.163).

became stable; however, the stress path stays at point B; this indicates that the soil reached the steady state, and that B is the steady state point.

Figure 7 illustrates the results of the undrained triaxial test for typical dilative sand. It is observed that the deviator stress increases with the axial strain until the strain approaches approximately 15%; after that, the slope of the stress-strain curve becomes flat. The induced excess pore water pressure increases slightly at very small strain until peak point A is reached, and then it drops off. Point A is also defined as the point of phase transform (Vaid and Chern, 1985). In Fig. 7(c), point A is a turning point on the stress path; after point A, the stress path approaches a specific line, which is called the line of the steady state failure envelope. After passing A, both the deviator stress and excess pore water pressure become stable, so that point B is a steady state point.

The results of the drained triaxial test for typical dilative sand are shown in Fig. 8. In comparison with the previous results of the undrained triaxial test, it is found that (1) the deviator stress increases to the peak point and then drops off; (2) a minor volumetric contraction occurs at the beginning; and when the strain approaches point A, the volume change alters from

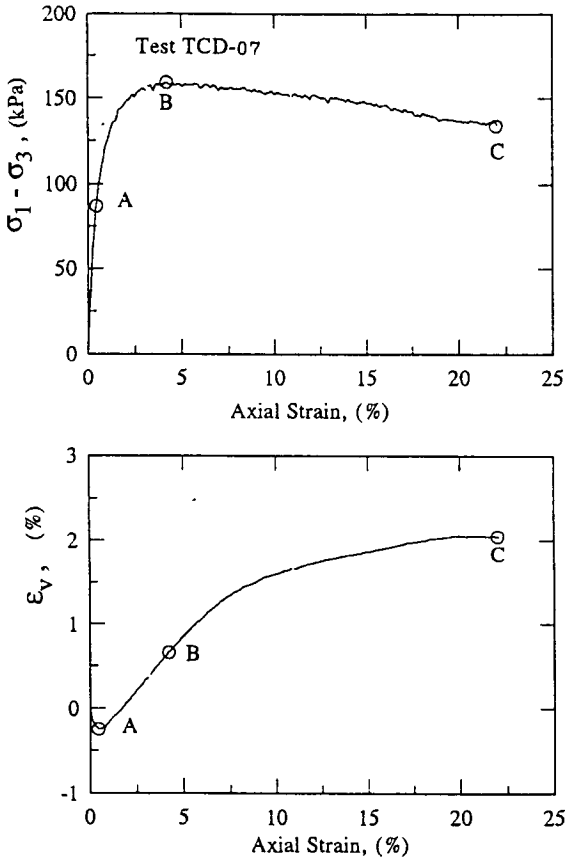

Fig. 8. Drained triaxial test with dilative response (D_r=62.8%, σ'_c=49 kPa, ψ=−0.153).

contractive to dilative; therefore, point A is regarded as a point of phase transformation. The increment of the volumetric dilation becomes moderate with respect to the increment of the axial strain and then approaches a constant near point C, the point of critical state.

5. Steady State Line of Hydraulic Fill Sand

Undrained triaxial tests were performed on samples of Mailiao sand with various relative densities and confining pressures. It can be observed from the results that regardless of the initial conditions of the sample, the relationship between the void ratio, e, and the effective mean principal stress, p', is linear in a semi-logarithmic diagram under steady state. This line, shown in Fig. 9, is called a steady state line. As there was no volume change in the undrained test, the e-logp' curve moves horizontally. If the initial state falls on the left side of the steady state line, the stress path will move to the right and show a dilative behavior. On the other hand, if the initial state falls on the right side of the steady state line, the stress path will move to the left and show a contractive behavior.

Corresponding to the steady state line obtained from the undrained triaxial test, a critical state line is defined as the e-log p' curve obtained from the drained triaxial test, as shown in Fig. 10. In Fig. 11, the drained

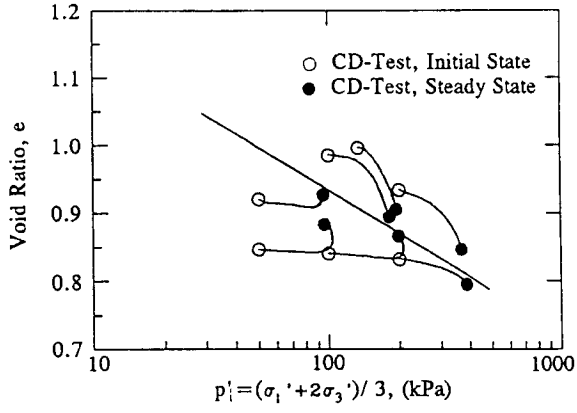

Fig. 10. Steady state of CD-tests (Mailiao sand).

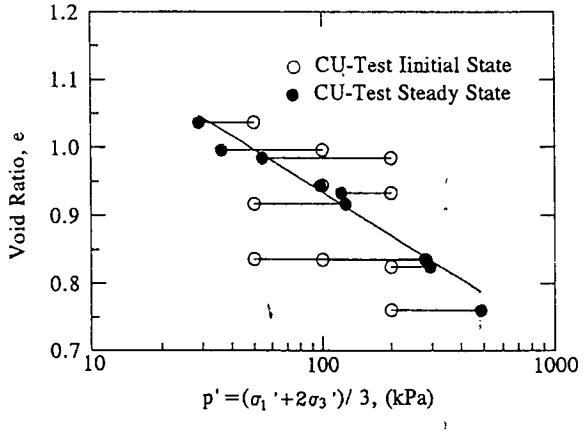

Fig. 9. Steady state of CU-test (Mailiao sand).

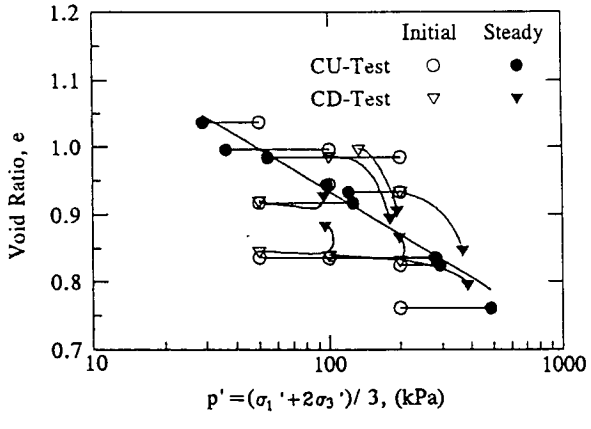

Fig. 11. Steady state of CU&CD-test (Mailiao sand).

and undrained test results in Figs. 9 and 10 are combined. It is found that almost all the data fall along the same line. This finding is consistant with that of Been *et al.* (1991). Consequently, it is suggested that the critical state line coincides with the steady state line regardless of the initial stress and void ratio conditions and drainage conditions during shearing.

The steady state lines obtained from the triaxial compression tests which were performed on samples of Yunlin sand prepared using the hydraulic transportation method and wet tamping method are shown in Fig. 12. It appears that the steady state line obtained from the wet tamping specimens shows lower steady-state strength than that from the hydraulic transportation specimens. The results from the axial extension tests, which are also included in the figure, indicate that the steady state line of the extension tests falls on the left side of those from the axial compression tests for the same void ratio; this means that the steady-state strength obtained from the extension tests is weaker than that from the compression tests. This reflects that the stress path does influence the steady state result, which is consistent with the conclusions drawn by Vaid *et al.* (1990) but is different from the result of Been *et al.* (1991). This discrepancy may be due to the difference of fabric obtained using various sample preparation methods with respect to the principal stress direction; more details will be discussed later.

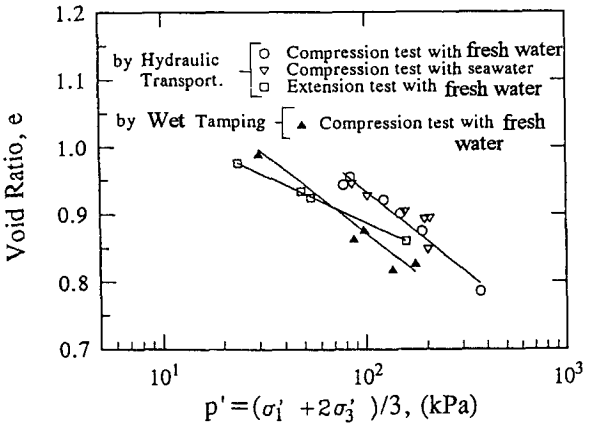

Fig. 12. Steady state line obtained using different methods (Yunlin sand).

Regarding the influence of the salinity of the pore fluid, as shown in Fig. 12, although the deviator stress of the specimen with fresh water fluid is higher than that with seawater fluid, the excess pore water pressure in the former specimen is also higher. Thus, the combined effect for different pore fluids, fresh water and seawater, possess identical steady state lines.

The steady state line in the e-logp' diagram can be expressed as

$$e=\Gamma-\lambda\log p', \tag{1}$$

where $p'=1/3\ (\sigma_1'+2\sigma_3')$, p' is the effective mean principal stress, σ_1' and σ_3' are major and minor principal stresses of the triaxial test, respectively, Γ is the reference void ratio under 1 kPa of p', and λ is the slope of the steady state line. From the results in Fig. 12, a summary of the steady state line equations for different sands and different conditions is given in Table 2. Comparing the λ value in Table 2 for Yunlin sand obtained from compression and extension tests, it is found that the slope of the steady state lines obtained from the sample prepared using both the hydraulic transportation method and the wet tamping method are almost the same, but that the steady-state strength of the former is higher than that of the latter. This is possibly due to the difference of fabric orientation between these two groups of samples, which will be discussed later.

Table 2. Steady State Line Equations of Different Kinds of Sand under Each Condition

Testing Sand	Fine Content	Preparation Method	Testing Type	Steady State Line Equations	Correlation Coefficient
Mailiao	0%	M. T.[a]	Com.[c]	e=0.9333−0.2109 log p'	0.971
Yunlin	0%	Hy. Transp.[b]	Com.	e=1.4175−0.2419 log p'	0.984
Yunlin	0%	Hy. Transp.	Ext.[d]	e=1.1686−0.1407 log p'	0.999
Yunlin	0%	M. T.	Com.	e=1.3467−0.2374 log p'	0.938
Yunlin	10%	M. T.	Com.	e=1.3125−0.2514 log p'	0.970
Yunlin	20%	M. T.	Com.	e=1.2806−0.2653 log p'	0.979
Yunlin	30%	M. T.	Com.	e=1.3546−0.3311 log p'	0.974

[a]Wet Tamping
[b]Hydraulic Transport
[c]Compression
[d]Extension.

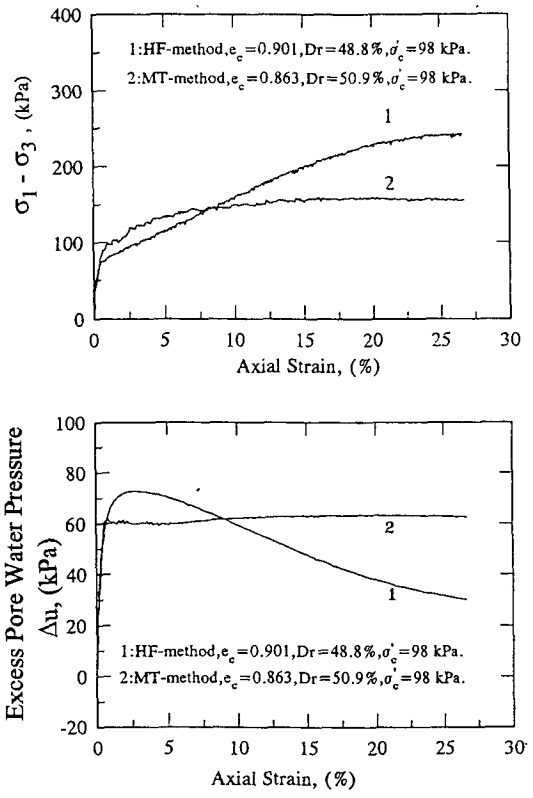

Fig. 13. Compression CU-test with different sample preparation methods.

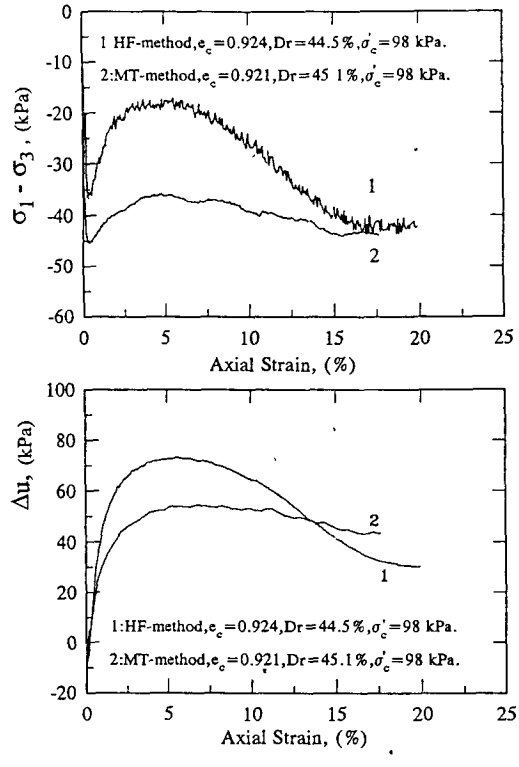

Fig. 14. Extension CU-test under different methods.

Figure 13 shows two sets of undrained triaxial compression test results with similar relative density (D_r=48.8% and 50.9%) but prepared using different methods. For the sample prepared using the hydraulic transportation method, the tendency of strain hardening is obvious because the deviator stress increases with respect to the increment of the strain. At the same time, the excess pore water pressure increases to a maximum value and then gradually drops off. Although it did not reach a clealy defined steady state, the deviator stress and the excess pore water pressure variation were minimal towards the end of test, which is a quasi steady state. For the sample prepared using the wet tamping method, both the deviator stress and the excess pore water pressure become gentle with regard to the increment of the strain. In other words, steady state is evidently reached. For the undrained triaxial extension tests, with the same confining pressure of 98 kPa, performed on these two kinds of samples, it can be found from Fig. 14 that the obtained deviator stress from the sample prepared using hydraulic transportation is less than that obtained using wet tamping. From the previous description, it can be summarized that the steady-state strength from the compression test was larger than that from the extension test. The steady-state strength was smaller for the samples prepared using hydraulic transportation than for those using wet

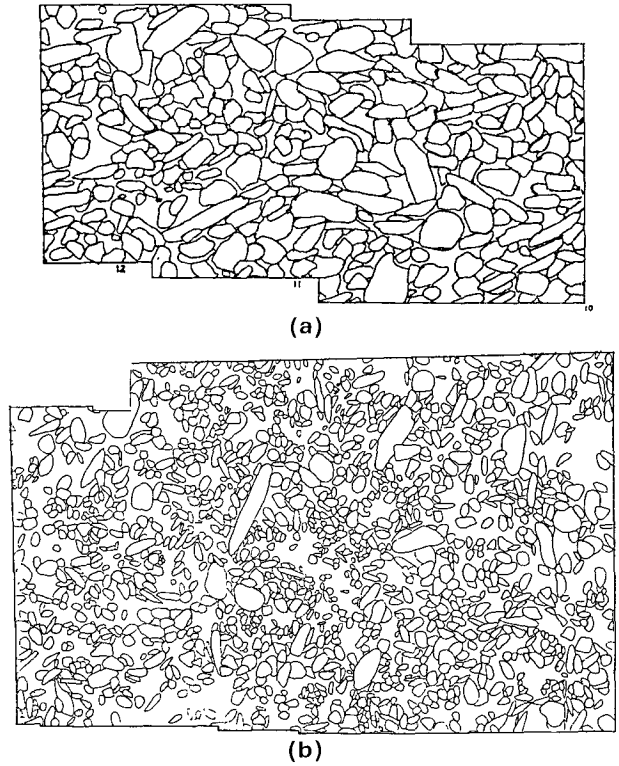

Fig. 15. Particle stacking results observed from vertical thin section. (a) Hydraulically transported specimen. (b) Wet tamping specimen.

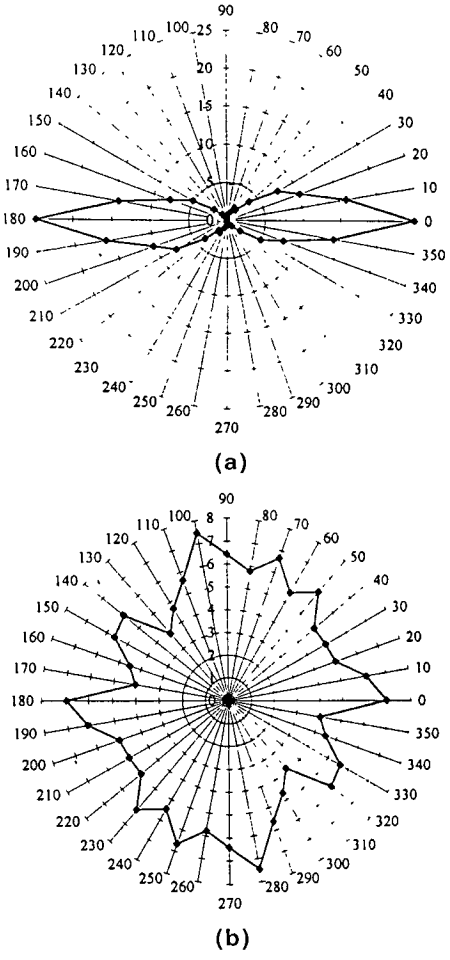

Fig. 16. Particle long axes orientation diagram of vertical thin section. (a) Hydraulic transportation. (b) Wet tamping specimen.

tamping. This might have been due to the difference of soil fabric obtained using these two different preparation methods. The sample prepared using the hydraulic transportation method possessed inherent particle orientation; thus, the long axis of the particles tended to be horizontal during sedimentation. This phenomenon can be verified from the particle stacking results and particle orientation diagram observed from the thin section using a microscope, given in Figs. 15 and 16. It is shown that the orientation of particle long axis of the specimens prepared using hydraulic transportation tended to be 0° and 180° (i.e., horizontal direction). For the hydraulic transported specimen, the resistance to axial compression was higher because the axis of the maximum principal stress was in vertical direction. On the other hand, when loading was extension, the axis of the major principal stress was in the horizontal direction, which was in the same direction as that of the long axis of the particles, and that is the reason why the steady-state strength was

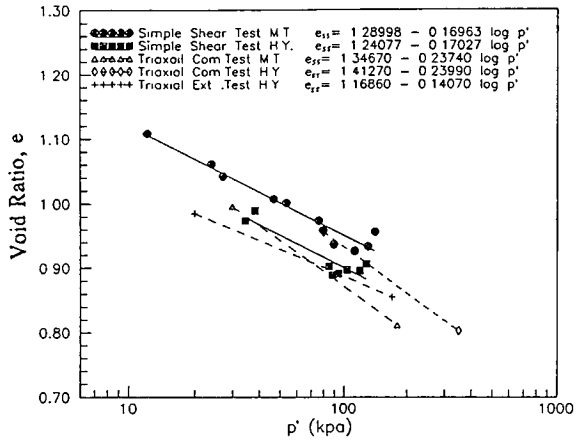

Fig. 17. Comparison of steady state lines between simple shear test and triaxial test.

weaker. On the other hand, the particle orientation for the samples prepared using wet tamping was more random and uniform in general for the later case. Therefore, the difference of the steady-state strength between compression and extension was not as obvious as it was in the hydraulic transported specimens.

According to the previous results, the fabric orientation of specimens with respect to the shearing modes may have resulted in different steady state lines. This phenomenon can be further verified by the results obtained from the simple shear test, as shown in Fig. 17. It is observed that two distinct steady state lines for the specimens prepared using different methods were obtained. The slope of these two lines is the same, this is, identical to the results from triaxial tests. Moreover, the position of the steady state line corresponding to the hydraulic transportation condition is lower than that of the wet tamping condition. This shows that in

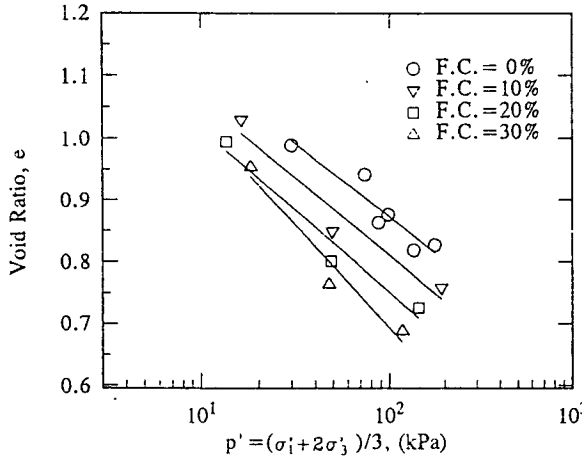

Fig. 18. Steady state lines with various fines content (F.C.).

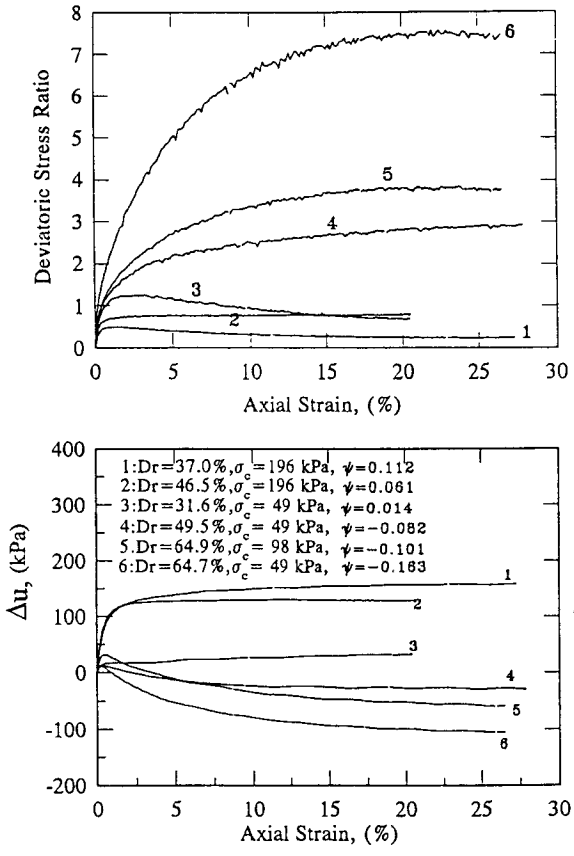

Fig. 19. Undrained response vs. ψ-value (Mailiao sand).

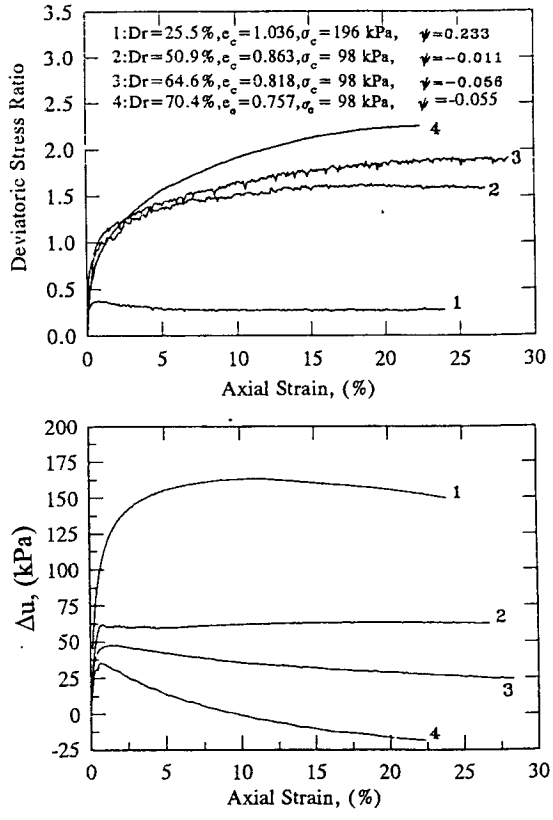

Fig. 20. Undrained response vs. ψ-value (Yunlin sand).

the horizontal simple shearing test, the steady-state shearing strength of the hydraulic transported specimen was smaller than that of the wet tamping specimens. This can also be attributed to the fabric orientation with respect to the direction of the applied shearing stress, which is the same reasoning stated above.

In this research, samples with different fines content were prepared using the wet tamping method, with which it is easier to generate samples with larger quantities of fines content. The steady state results are illustrated in Fig. 18 and Table 2. It is observed that the slope of the steady state line increases with the fines content. The position of the steady state line moves to the left and downward with the fines content. This means that, for fines contents up to 30%, the increase of the fines content produces higher compressibility and lower steady-state strength.

6. State Parameter and Engineering Characteristics

As stated in the previous sections, regardless of the initial conditions of the sample, the relationship between the void ratio and the mean effective principal stress approaches the steady state line. A state parameter is defined by Been and Jefferies (1985) as the difference of the void ratio between current state and steady state under identical average principal stress. That is,

$$\psi = e_0 - e_{ss}, \tag{2}$$

where e_0 is the void ratio in current state, and e_{ss} is the steady state void ratio in the identical principal stress.

The results of the undrained tests with various state parameters and mechanical properties on Mailiao sand and Yunlin sand are shown in Figs. 19 and 20. The initial state is above the steady state line when the state parameter is positive and the soil is contractive. Positive excess pore water pressure is generate when it is sheared, and the soil is more susceptible to liquefaction. A large, positive ψ value cooresponds to more contractive behavior or a higher value of the excess pore water pressure during shearing. In the case of the drained triaxial test, as shown in Fig. 21, the contraction in volumetric strain is proportional to the ψ value.

In summary, the tendency of the volume change and variation of the excess pore water pressure can be fully described with respect to state parameter. From

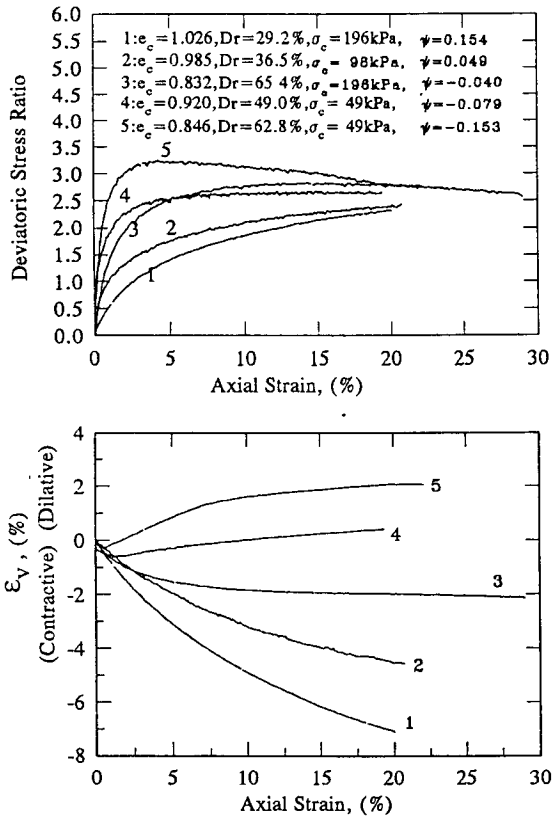

Fig. 21. Drained test response vs. ψ-value (Mailiao sand).

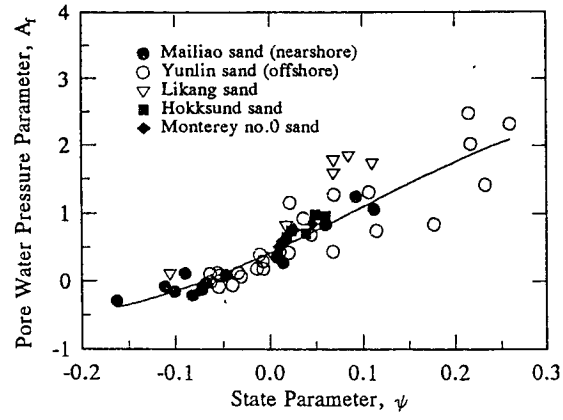

Fig. 22. Pore pressure parameter vs. state parameter.

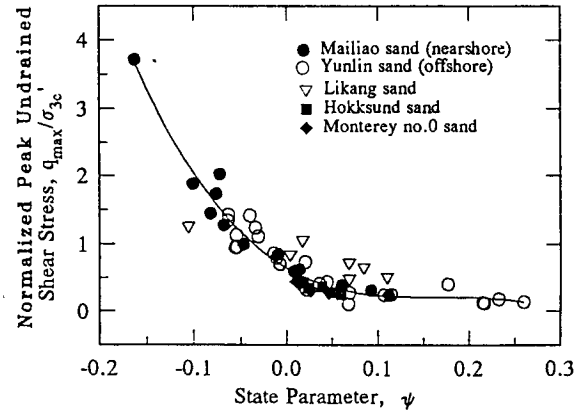

Fig. 23. Undrained shear strength vs. state parameter.

the stress-strain relationship point of view, it is easy to predict the potential for strain softening and flow failure based on the state parameter.

Using the concept of the state parameter, distinct steady state lines can be correlated with the engineering properties for various kinds of sand. Figures 22 and 23 show the results of the normalized undrained shear resistance and excess pore water pressure parameter with respect to the state parameter for Mailiao sand and Yunlin sand. When compared with the results for other kinds of sand obtained by Jiang (1994) and Been *et al.* (1991), which are also illustrated in the figures, it seems that the relationship between the state parameter and the engineering properties is also applicable to flat sand. In other words, the state parameter is independent of the particle shape. From the results of the drained triaxial test shown in Figs. 24 and 25, it is also found that the state parameter is related to the friction angle (φ') as well as the volumetric dilation rate ($d\varepsilon_v/d\varepsilon_a$). It is observed from the figure that the soil tends to be contractive when state parameter is positive; therefore, the volumetric dilation rate is small while the dilation effect is obvious when the state parameter is negative; in this case, the effective friction angle tends to be larger.

The results obtained in this research are compared with those of Been *et al.* (1991) in Figs. 24 and 25. A similar trend can be found except that the effective internal friction angle of the sand obtained in this research seems to be a little higher.

The cone penetration test (CPT) is a kind of field test which is widely applied to reclamation engineering. Been *et al.* (1987, 1991) generated a correlation equation to describe the state parameter in terms of the penetration resistance of CPT (q_c) from results of laboratory calibration chamber tests performed on six different kinds of sand. This equation is expressed as follows :

$$\psi = \frac{-1}{(8.1 - \ln\lambda)} \times \ln\left[\frac{q_c - p}{p'}\left(8 + \frac{0.55}{\lambda - 0.01}\right)^{-1}\right], \quad (3)$$

where p is the total mean principal stress. Substituting the λ value obtained from this research into Eq. (3),

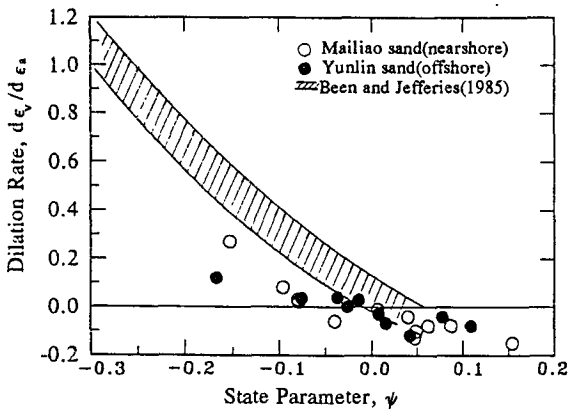

Fig. 24. Dilation rate vs. state parameter.

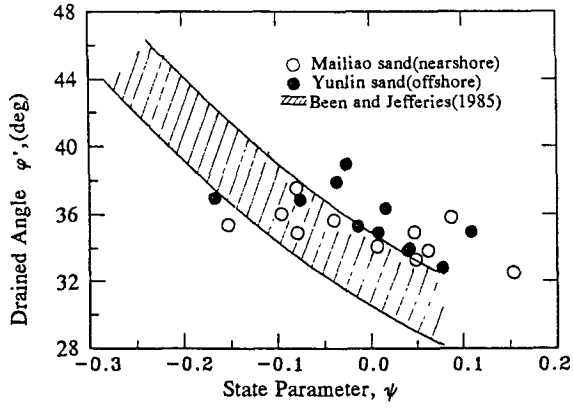

Fig. 25. Drained friction angle vs. state parameter.

the value of $(q_c-p)/p'$ is described in terms of the state parameter for the sand used in this research as follows:

$$\frac{q_c-p}{p'} = 10.423e^{-9.540\psi}. \quad \textbf{(4)}$$

The curves determined using this equation for Yunlin sand are plotted in Fig. 26 along with the curves obtained by Been *et al.* It is found from Fig. 26 that the positions of the curves from Yunlin sand are lower than those of the other curves. This phenomenon can be explained by the fact that the value of the only parameter in Eq. (3), λ_{ss}, the slope of the steady state line, which is 0.237 for Yunlin sand, is larger than the values that Been *et al.* obtained which ranged from 0.028 to 0.170. The same result was also obtained for Yunlin sand with a fines content of 30%, λ_{ss}=0.332, so that the curve obtained falls below the curve from clean sand with zero fines content. This means that, for the same q_c value, the steeper the steady state line, the smaller the ψ value will be. Thus, the in situ state parameter can be obtained using Eq. (4) and Fig. 26 if the q_c value from CPT were achieved. Moreover, the behavior during shearing and its related mechanical characteristics for each soil stratum can also be estimated indirectly using the stated procedure.

III. Conclusions

In this research, a series of strain controlled triaxial tests have been performed on samples using the hydraulic transportation method or wet tamping method for both flat shaped Mailiao sand and Yunlin sand to study the steady state of sands with regard to the effect of all the related factors. Furthermore, based on the steady state, the state parameters have been computed and the relation concerned with mechanical characteristics discussed. Referring to the results obtained, the following conclusions can be made:

(1) The samples prepared using the hydraulic transportation method in this research met the requirements for uniformity and repeatability.

(2) The variations of the initial void ratio, confining pressure, drainage condition and pore fluid had no significant effect on the steady state line. Critical state and steady state may be regarded as the same for the sands tested.

(3) The slope of the steady state lines obtained from tests performed on the specimens prepared using the hydraulic transportation method and wet tamping method are identical. However, the compressive steady-state strength of the specimens from hydraulic transportation sand appears to be higher. This results in two distinct steady state lines obtained from these two groups of

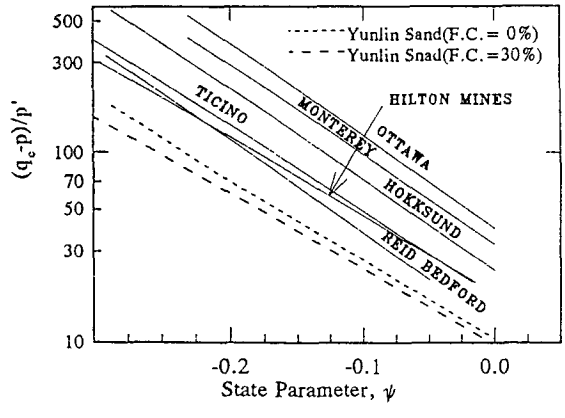

Fig. 26. CPT penetration resistance vs. state parameter

specimens.

(4) For specimens prepared using the hydraulic transportation method, the position of the steady state line obtained from the extension test is lower than that obtained from the compression test. This means that the strength at steady state from the extension test is smaller than from the compression test.

(5) For the flat sand used in this research, both the sample preparation method and stress path (compression or extension) influenced the steady state results, which might be attributable to the difference of fabric orientation with respect to major principal stress direction.

(6) The deviatoric stress of the specimen with fresh water fluid was higher than that with saline water fluid, and the excess pore water pressure in the former specimen was also higher. Thus, the combined effect resulted in identical steady state lines.

(7) The slope of the steady state line was steeper when the fines content increased, and the steady-state strength was reduced.

(8) Application of the state parameter to evaluate the engineering properties of flat shaped hydraulic fill sand is possible. The correlated curves obtained from different sands under various conditions seem to be consistent.

Acknowledgment

Financial support from National Science Council (NSC 82-0115-E008-175) and the Sinotech Foundation for Research and Development of Engineering Sciences and Technologies as well as specimens provided by Sinotech Engineering Consultants, Inc. are gratefully appreciated.

References

Been, K. and M. G Jefferies (1985) A state parameter for sands. *Geotechnique*, **35**(2), 99-112.

Been, K., M. G. Jefferies, J. H. A. Crooks, and L. Rothenburg (1987) The cone penetration test in sands: part (2) general inference of state. *Geotechnique*, **37**(3), 285-299.

Been, K., M. G. Jefferies, and J. Hachey (1991) The critical state of sands. *Geotechnique*, **41**(3), 365-381.

Jiang, M. S. (1994) *Using State Parameter to Evaluate the Deformation Behavior of Sandy Soil* (in Chinese). M.S. Thesis. Department of Civil Engineering, National Central University, Chung Li, Taiwan, R.O.C.

Li, J. C., L K. Chien, and C. J. Jeng (1991) Dynamic deformation characteristics of granular soil with initial static shear stresses (in Chinese). *Journal of the Chinese Institute of Civil and Hydraulic Engineering*, **3**(4), 309-319.

Sladen, J. A. and K. J. Wemitt (1989) Influence of placement method on the in situ density of hydraulic sand fills. *Canadian Geotechnical Journal*, **26**, 453-466.

Vaid, Y. P. and J. C. Chern (1985) Cyclic and monotonic undrained response of saturate sand. In: *Proceedings of ASCE Convection, Session on Advances in the Art of Testing Soils Under Cyclic Conditions*, pp. 120-147. V. Khosla, Ed. Detroit, MI, U.S.A.

Vaid, Y. P., E. K. F. Chung, and R. H. Kuerbis (1990) Stress path and steady state. *Canadian Geotechnical Journal*, **27**(1), 1-7.

Verhoeven, F. A., A. J. de Jong, and P. Lubking (1988) The essense of soil properties in today's dredging technology. In: *Hydraulic Fill Structures, Geotechnical Special Publication*, No. 21, pp. 1033-1064. A Specialty Conference Sponsored by the Geotechnical Engineering Division of the American Society of Civil Engineers, Colorado State University, Fort Collins, CO, U S.A.

Characteristics of Flat Hydraulic Fill Sand

扁平狀水力填築砂土之力學特性

李建中　鄭清江

國立中央大學土木工程研究所

摘　要

國內目前正規畫在西海岸開發許多離島工業區及海埔新生地，且大部份擬採用抽取附近海床砂土來填築。因此有關水力填築技術及相關之大地工程問題將成爲當前重要之研究課題。

本研究運用過程模擬方式製作了水力輸砂儀，以作爲試驗用片狀砂土的模擬水力輸砂試體之準備方式。針對此種模擬試體沈積過程中之行爲做詳細探討，最後並以沈積完成之試體，進行片狀水力填築砂土穩定狀態線及狀態參數與工程特性之關係作廣泛研究。

研究結果顯示，以水力輸砂儀製作之試體，可滿足一般模擬試體均勻性與可重複性的要求。不同孔隙介質對穩定狀態線的影響不大。在本片狀砂土情況下，水力輸砂儀製作之試體，其試驗結果所得之穩定狀態線的斜率與濕搗 法製作試體之結果相近似，惟在相同孔隙比下前者之壓縮剪力強度略高於後者；且在同樣水力輸砂試體下，由伸張試驗所得之穩定狀態線顯示其穩定狀態剪力強度較壓縮試驗結果爲低。此係受試體組構與應力方向關係所影響。砂土中細料含量增加，穩定狀態線斜率變陡，強度則隨細料的增加而降低。利用狀態參數作爲評估片狀水力填築砂土工程特性，可在不同砂土種類及狀態下，獲得其關係曲線相當程度之一致性。